Inorg. Chem. **2005**, *44*, 8399–8406

Hexacyanocobaltate(III) Anions as Precursors of Co(II)–Ni(II) Cyano-Bridged Multidimensional Assemblies: Hydrothermal Syntheses, Crystal and Powder X-ray Structures, and Magnetic Properties

A. Rodriguez,[†] H. Sakiyama,[‡] N. Masciocchi,[§] S. Galli,*[,§] N. Gálvez,[†] F. Lloret,[||] and E. Colacio*[,†]

Departamento de Química Inorgánica, Universidad de Granada, Avenida Fuentenueva s/n, 18071 Granada, Spain, Department of Material and Biological Chemistry, Faculty of Science, Yamagata University, Kojirakawa, 1-4-12, Yamagata 990-8560, Japan, Dipartimento di Scienze Chimiche e Ambientali, Università dell'Insubria, Via Valleggio 11, 22100 Como, Italy, and Departament de Química Inorgánica, Facultad de Química, Universidad de Valencia, E-46100 Burjassot, Valencia, Spain

Received July 13, 2005

Three novel cyanide-bridged heterobimetallic coordination polymers have been synthesized by hydrothermal routes, in superheated water solutions, by using $K_3[Co(CN)_6]$, $NiCl_2 \cdot 6H_2O$, and α-diimine ligands: $[Ni(CN)_4Co(phen)]$ (**1**; phen = 1,10-phenanthroline), $[Ni(CN)_4Co(2,2'\text{-bipy})]$ (**2**; 2,2′-bipy = 2,2′-bipyiridine), and $[Ni(CN)_4Co(2,2'\text{-bipy})_2]$ (**3**). The isostructural compounds **1** and **2** contain a two-dimensional network with Co(II) centers octahedrally coordinated by one chelating 2,2′-bipy ligand and four cyanide groups of four distinct $[Ni(CN)_4]^{2-}$, through crystallographically equivalent, bridging units. Compound **3** contains one-dimensional zigzag chains in which the Co(II) ion is coordinated by two chelating 2,2′-bipy ligands and two cyanides from two different $[Ni(CN)_4]^{2-}$ units cis to each other. These compounds have been fully characterized by single-crystal or unconventional powder X-ray diffraction analyses and variable-temperature magnetic measurements.

Introduction

In recent years, cyanide-bridged metal-coordination polymers have deserved special attention because they exhibit, among others, interesting electrochemical, zeolitic, magnetic, and photomagnetic properties.[1] Most of these systems have been prepared by controlled assembly reactions of cyanide or cyanide-containing metal complexes with metal ions or metal complexes with available coordination sites. Nevertheless, the number of cyano-bridged coordination polymers prepared from less-controlled hydrothermal reactions has dramatically increased during the past decade. In this regard, a great variety of cyano-bridged extended networks, in which organic and/or cyanide ligands act as linkers between copper centers, have been prepared from CuCN and organic multitopic ligands containing nitrogen donor atoms.[2]

Recently, we[3] and others[4] have shown that cyanide-bridged bimetallic coordination polymers can also be assembled through hydrothermal reactions by using the hexacyanoferrate(III) anion as a source of cyanide groups, which act as both reducing agents and bridging ligands. In an attempt to prepare cyano-bridged Co(II)−Ni(II) bimetallic assemblies, we have decided to use the hexacyanocobaltate(III) anion as a precursor. We report hereafter, as a result, the hydrothermal syntheses of three novel coordination polymers: $[Ni(CN)_4Co(phen)]$ (**1**; phen = 1,10-phenanthroline), $[Ni(CN)_4Co(2,2'\text{-bipy})]$ (**2**; 2,2′-bipy = 2,2′-bipyridine), and $[Ni(CN)_4Co(2,2'\text{-bipy})_2]$ (**3**), together with their structural characterizations, including unconventional X-ray powder diffraction (XRPD) methods for **2**, and their magnetic properties.

Experimental Section

Materials. Nickel(II) chloride hexahydrate (99.99%), 2,2′-bipyridine (99+%), and 1,10-phenanthroline (99+%) were purchased from Aldrich and were used without further purification. Potassium hexacyanocobaltate(III) was prepared by adding an excess of potassium cyanide to a solution of a soluble cobalt salt and allowing for the slow crystallization of the product on standby.

Synthesis of $[Ni(CN)_4Co(phen)]$ (1). A mixture of $NiCl_2 \cdot 6H_2O$ (0.143 g, 0.6 mmol), $K_3[Co(CN)_6]$ (0.200 g, 0.6 mmol), 1,10-

* To whom correspondence should be addressed. E-mail: simona.galli@uninsubria.it (S.G.), ecolacio@ugr.es (E.C.).
[†] Universidad de Granada.
[‡] Yamagata University.
[§] Università dell'Insubria.
[||] Universidad de Valencia.

10.1021/ic0511672 CCC: $30.25
Published on Web 10/06/2005

phenanthroline (0.108 g, 0.6 mmol), and distilled water (10 mL) was sealed in a Teflon-lined acid digestion autoclave and heated hydrothermally at 180 °C under autogenous pressure. After 2 h of heating, the reaction vessel was cooled for 2 h. Red pseudocubic crystals were obtained. Yield: 75% based on Ni.

Synthesis of [Ni(CN)$_4$Co(2,2′-bipy)] (2). This compound was obtained as dark red crystals through the same hydrothermal conditions as those for **1** by using $NiCl_2 \cdot 6H_2O$ (0.143 g, 0.6 mmol), $K_3[Co(CN)_6]$ (0.200 g, 0.6 mmol), 2,2′-bipyridine (0.094 g, 0.6 mmol), and distilled water (10 mL). Yield: 45% based on Ni.

Synthesis of [Ni(CN)$_4$Co(2,2′-bipy)$_2$] (3). Red pseudo-octahedral crystals of **3** were obtained from hydrothermal treatment of $NiCl_2 \cdot 6H_2O$ (0.143 g, 0.6 mmol), $K_3[Co(CN)_6]$ (0.200 g, 0.6 mmol), 2,2′-bipyridine (0.094 g, 0.6 mmol), and distilled water (10 mL) in the same conditions as those for **1** and **2** but prolonging the reaction up to 12 h under autogenous pressure. Yield: 35% based on Ni.

Physical Measurements. Elemental analyses were carried out at the Instrumentation Scientific Centre of the University of Granada on a Fisons−Carlo Erba analyzer model EA 1108. IR spectra were recorder on a MIDAC progress IR spectrometer using KBr pellets. Magnetization and variable-temperature (2−300 K) magnetic susceptibility measurements on polycrystalline samples were carried out in the 2−300 K temperature range with a Quantum Design SQUID MPMS XL-5 operating at different magnetic fields. Magnetic calculations were made using the MagSaki magnetic software program.[5]

Single-Crystal Structure Determination of 1 and 3. Suitable red crystals of **1** and **3** were mounted in air on the glass fiber tip of a goniometer head. The data collections were performed on a Bruker AXS APEX CCD area detector equipped with graphite-monochromatized Mo Kα radiation ($\lambda = 0.710\ 69$ Å) by applying the ω-scan method. Data reduction within the sphere with $2\theta < 56.51°$ (**1**) or $2\theta < 60.03°$ (**3**) afforded 8666 (**1**) or 4669 (**3**) reflections, of which 1742 (**1**) or 3322 (**3**) were unique and 1658 (**1**) or 1788 (**3**) were observed [$I > 2\sigma(I)$]. An empirical absorption correction was applied.[6] The structures were solved by direct methods[7] and refined with full-matrix least-squares calculations on F^2.[8] Anisotropic temperature factors were assigned to all atoms but hydrogens, riding their parent atoms with an isotropic temperature factor arbitrarily chosen as 1.2 times that of the parent itself. The final Co−N−C−Ni coordination of the cyanide groups has been assigned, at the refinement stage, considering three distinct models, namely, (i) Co−N−C−Ni, (ii) Co−C−N−Ni, and (iii) a disordered model, admitting both i and ii with 0.5 probability each and comparing the pertinent refinement agreement factors. Final R, wR_{wp}, and goodness of fit agreement factors, details on data collection, and analyses for **1** and **3** can be found in Table 1.

XRPD Analysis of [Ni(CN)$_4$Co(2,2′-bipy)]$_n$ 2. The powders were gently ground in an agate mortar and then deposited with care in the hollow of an aluminum holder equipped with a zero-background plate (supplied by *The Gem Dugout*, State College, PA). Diffraction data (Cu Kα, $\lambda = 1.5418$ Å) were collected on a θ:θ Bruker AXS D8 vertical scan diffractometer equipped with primary and secondary Soller slits, a secondary beam curved graphite monochromator, a Na(Tl)I scintillation detector, and pulse height amplifier discrimination. The generator was operated at 40 kV and 40 mA. Optics used are the following: divergence 0.5°, antiscatter 0.5°, receiving 0.2 mm. Nominal resolution of the present setup is 0.07° 2θ for the Si(111) peak at 28.44° (2θ, α_1 component). A long scan was performed with $5 < 2\theta < 105°$ with $t = 11$ s and $\Delta 2\theta = 0.02°$.

Indexing was obtained with the aid of TREOR[9] [monoclinic, $a = 6.61$ Å, $b = 16.84$ Å, $c = 12.12$ Å, $\beta = 90.80°$, $M(22)$[10] $= 28$, $F(22)$[11] $= 54$ (0.005, 85)]. Systematic absences indicated $C2/c$ as the probable space group, later confirmed by successful solution and refinement. The structure solution was performed by using the simulated annealing[12] technique implemented in Topas-R.[13] Both types of ligands were treated as rigid bodies, assigning average literature bond distances and angles (for the CN group, C−N = 1.15 Å; for the bipyridine moiety, C−C = C−N = 1.40 Å and C−H = 1.08 Å; ring bond angles = 120.0°). The Co−N−C−Ni coordination of the cyanide groups has been assigned on the basis of the results of the single-crystal determination on the isostructural compound **1**. The final refinements were performed by the Rietveld method using Topas-R, maintaining the rigid bodies described above. Peak shapes were described by the fundamental parameters approach.[14] The experimental background was fit by a polynomial description. Systematic errors were modeled with sample-displacement angular shifts, preferred orientation corrections in the March-

(1) (a) Dunbar, K. R.; Heintz, R. A. *Prog. Inorg. Chem.* **1997**, *45*, 283. (b) Verdaguer, M. *Science* **1996**, *272*, 698. (c) Entley, W.; Girolami, G. S. *Science* **1995**, *268*, 397. (d) Ferlay, S.; Mallah, T. M.; Ouahes, R.; Veillet, P.; Verdaguer, M. *Nature* **1995**, *378*, 701. (e) Verdaguer, M.; Bleuzen, A.; Marvaud, V.; Vaissermann, J.; Seuleiman, M.; Desplanches, C.; Scuiller, A.; Train, C.; Garde, R.; Gelly, G.; Lomenech, C.; Rosenman, I.; Veillet, P.; Cartier, C.; Villain, F. *Coord. Chem. Rev.* **1999**, *190*, 1023. (f) Fehlhammer, W. P.; Fritz, M. *Chem. Rev.* **1993**, *93*, 1243. (g) Ohba, M.; Okawa, K. *Coord. Chem. Rev.* **2000**, *198*, 313. (h) Marvilliers, A.; Parsons, S.; Rivière, E.; Audière, J. P.; Kurmoo, M.; Mallah, T. *Eur. J. Inorg. Chem.* **2001**, 1287 and references cited therein. (i) Parker, R. J.; Lu, K. D.; Batten, S. R.; Moubaraki, B.; Murray, K. S.; Spiccia, L.; Cashion, J. D.; Rae, A. D.; Willis, A. *J. Chem. Soc., Dalton Trans*. **2002**, 3723 and references cited therein. (j) Černák, J.; Orendáč, M.; Potočňák, I.; Chomič, J.; Orendáčová, A.; Skoršepa, J.; Feher, A. *Coord. Chem. Rev.* **2002**, *224*, 51 and references cited therein. (k) Kou, H.-Z.; Zhou, B. C.; Liao, D.-Z.; Wang, R. J.; Li, Y. *Inorg. Chem.* **2002**, *41*, 25 and references cited therein. (l) Chesnut, D. J.; Hagrman, D.; Zapf, P. J.; Hammond, R. P.; LaDuca, R.; Haushalter, R. C.; Zubieta, J. *Coord. Chem. Rev.* **1999**, *190*, 757 and references cited therein. (m) Chesnut, D. J.; Plewak, D.; Zubieta, J. *J. Chem. Soc., Dalton Trans.* **2001**, 2567. (n) Miller, J. S.; Manson, J. L. *Acc. Chem. Res.* **2001**, *34*, 563. (o) Lescouëzec, R.; Vaissermann, J.; Ruiz-Pérez, C.; Lloret, F.; Carrasco, R.; Julve, M.; Verdaguer, M.; Dromzée, Y.; Gatteschi, D.; Wernsdorfer, W. *Angew. Chem., Int. Ed*. **2001**, *40*, 1760. (p) Pilkington, M.; Decurtins, S. *Compr. Coord. Chem. II* **2004**, *7*, 177−229. (q) Figuerola, A.; Díaz, C.; Ribas, J.; Tangoulis, V.; Granell, J.; Lloret, F.; Mahía, J.; Maestro, M. *Inorg. Chem.* **2003**, *42*, 641.

(2) (a) Chesnut, D. J.; Plewak, D.; Zubieta, J. *J. Chem. Soc., Dalton Trans*. **2001**, 2567. (b) Chesnut, D. J.; Kusnetzow, A.; Birge, R.; Zubieta, J. *J. Chem. Soc., Dalton Trans*. **2001**, 2581. (c) Chesnut, D. J.; Kusnetzow, A.; Birge, R.; Zubieta, J. *Inorg. Chem.* **1999**, *38*, 5484. (d) Chesnut, D. J.; Kusnetzow, A.; Zubieta, J. *J. Chem. Soc., Dalton Trans.* **1998**, 4081. (e) Chesnut, D. J.; Zubieta, J. *J. Chem. Soc., Chem. Commun*. **1998**, 1707.

(3) (a) Colacio, E.; Domínguez-Vera, J. M.; Lloret, F.; Moreno-Sánchez, J. M.; Kivekäs, R.; Rodríguez, A.; Sillanpää, R. *Inorg. Chem.* **2003**, *42*, 4209. (b) Colacio, E.; Debdoubi, A.; Kivekäs, R.; Rodríguez, A. *Eur. J. Inorg. Chem.* **2005**, 2860.

(4) Yu, J.-H.; Xu, J.-Q.; Yang, Q.-X.; Pan, L.-Y.; Wang, T.-G.; Lü, C.-H.; Ma, T.-H. *J. Mol. Struct.* **2003**, *658*, 1.

(5) Sakiyama, H. MagSaki, Sakiyama Laboratory, 2000.

(6) Sheldrick, G. M. *SADABS, Program for Empirical Absorption Correction*; University of Göttingen: Göttingen, Germany, 1996.

(7) Altomare, A.; Cascarano, G.; Giacovazzo, C.; Guagliardi, A.; Moliterni, A. G. G.; Burla, M. C.; Polidori, G.; Cavalli, M.; Spagna, R. *SIR97: package for structure solution by direct methods*; University of Bari: Bari, Italy, 1997.

(8) Sheldrick, G. M. *SHELX97: program for crystal structure refinement*; University of Göttingen: Göttingen, Germany, 1997.

(9) Werner, P. E.; Eriksson, L.; Westdahl, M. *J. Appl. Crystallogr.* **1985**, *18*, 367.

(10) De Wolff, P. M. *J. Appl. Crystallogr.* **1968**, *1*, 108.

(11) Smith, G. S.; Snyder, R. L. *J. Appl. Crystallogr.* **1979**, *12*, 60.

(12) Coelho, A. A. *J. Appl. Crystallogr.* **2000**, *33*, 899.

(13) Topas-R, Bruker AXS: General profile and structure analysis software for powder diffraction data.

(14) Cheary, R. W.; Coelho, A. A. *J. Appl. Crystallogr.* **1992**, *25*, 109.

Table 1. Crystal Data and Refinement Details for Compounds **1**−**3**

compound	[Ni(CN)$_4$Co(phen)], **1**	[Ni(CN)$_4$ Co(2,2′-bipy)], **2**	[Ni(CN)$_4$Co(2,2′-bipy)$_2$], **3**
formula	$C_{16}H_8CoN_6Ni$	$C_{14}H_8CoN_6Ni$	$C_{24}H_{16}CoN_8Ni$
fw, g mol^{-1}	401.92	377.88	534.07
system	monoclinic	monoclinic	orthorhombic
space group	*C*2/*c*	*C*2/*c*	*Pbcn*
a, Å	6.5604(4)	6.6089(2)	14.1128(45)
b, Å	19.1843(12)	16.8495(6)	10.1585(22)
c, Å	11.6414(8)	12.1193(5)	15.8185(33)
β, deg	91.072(1)	90.782(2)	90
V, Å^3	1464.9(2)	1349.4(1)	2267.8(1)
Z	4	4	4
ρ_{calc}, g cm^{-3}	1.822	1.859	1.564
F(000)	804	756	1084
μ, mm^{-1}	2.43 (Mo Kα)	11.4 (Cu Kα)	1.59 (Mo Kα)
diffractometer	Bruker Apex	Bruker D8 Advance	Bruker Apex
T, K	298(2)	298(2)	298(2)
indexing method		TREOR90[9]	
Indexing FoM		$M(22)$[10] = 28	
		$F(22) = 54(0.005, 85)$	
2θ range, deg	4.2−56.5	5−105	4.9−60.0
N_{data}	1742 indep F_o	5001 y_o	3322 indep F_o
N_{obs}	1658 indep $F_o > 4\sigma(F_o)$	794 F_o	1788 indep $F_o > 4\sigma(F_o)$
FOMs	0.024, 0.055[a]	0.101, 0.132[b]	0.116, 0.164[a]
R_{Bragg}[c]		0.049	
GOF	1.091[d]	1.302[e]	1.049[d]
V/*Z*′, Å^3	336.2	337.4	566.9
highest peak (e^{-1} Å^3)	0.34		0.98
deepest hole (e^{-1} Å^3)	−0.26		−0.58
pref. orient. pole		[1, 1, 1]	

[a] $R(F)_{all} = \sum||F_o| - |F_c||/\sum|F_o|$, $wR(F^2)_{all} = [\sum w(F_o^2 - F_c^2)^2/\sum wF^4]^{1/2}$. [b] $R_p = \sum_i|y_{i,o} - y_{i,c}|/\sum_i|y_{i,o}|$, $R_{wp} = [\sum_i w_i(y_{i,o} - y_{i,c})^2/\sum_i w_i(y_{i,o})^2]^{1/2}$. [c] $R_{Bragg} = \sum_n|I_{n,o} - I_{n,c}|/\sum_n I_{n,o}$. [d] $S(F^2) = [\sum w(F_o^2 - F_c^2)^2/(n-p)]^{1/2}$. [e] $\chi^2 = \sum_i w_i(y_{i,o} - y_{i,c})^2/(N_{obs} - N_{par})$, with F_o and F_c the observed and calculated structure factors, n and p the number of reflections and refined parameters, $y_{i,o}$ and $y_{i,c}$ the observed and calculated profile intensities, and $I_{n,o}$ and $I_{n,c}$ the observed and calculated Bragg reflections, respectively, $w = 1/[\sigma^2(F_o^2) + (0.019P)^2 + 1.88P]$, where $P = (F_o^2 + 2F_c^2)/3$ and $w_i = 1/y_{i,o}$.

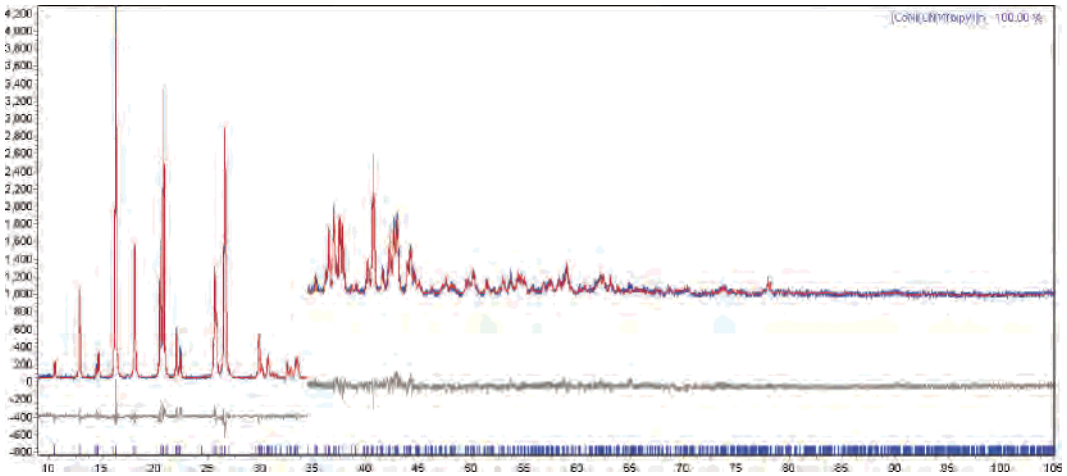

Figure 1. Rietveld refinement results for **2** as appreciable from experimental, calculated, and difference diffraction patterns. Peak markers are at the bottom. For the sake of clarity, the portion above 35° has been magnified (3×). Horizontal axis: 2θ, deg. Vertical axis: counts.

Dollase[6] formulation (with a [111] pole), and anisotropic peak shape broadening.[15] Metal atoms were given a refinable, isotropic displacement parameter (B_M), while lighter atoms were assigned a common $B = B_M + 2.0$ Å^2 value. Scattering factors, corrected for real and imaginary anomalous dispersion terms, were taken from the internal library of Topas-R.

Final R_p, R_{wp}, R_{Bragg}, and χ^2 agreement factors, details on data collection, and analyses can be found in Table 1. Figure 1 shows the final Rietveld refinement plot.

Crystallographic data (excluding structure factors) for the reported structures have been deposited with the Cambridge Crystallographic Data Centre as supplementary publications No. CCDC 276881−276883. Copies of the data can be obtained free of charge upon application to CCDC, 12 Union Road, Cambridge CB2 1EZ, U.K. (fax, (+44)1223 336-033; e-mail, deposit@ccdc.cam.ac.uk).

(15) (a) March, A. *Z. Kristallogr.* **1932**, *81*, 285. (b) Dollase, W. A. *J. Appl. Crystallogr.* **1987**, *19*, 267.

Results and Discussion

Hydrothermal reactions in the presence of organic components have been demonstrated to be a versatile technique for the synthesis of new materials with a variety of structural architectures. The reduced viscosity of the solvent under these conditions favors the solvent extraction of solids, the self-assembly of the precursors, and the crystal growth from the solution. Hydrothermal reactions between [Fe(CN)$_6$]$^{3-}$ and Cu(II) ions have led, in some cases, to fully reduced cyano-

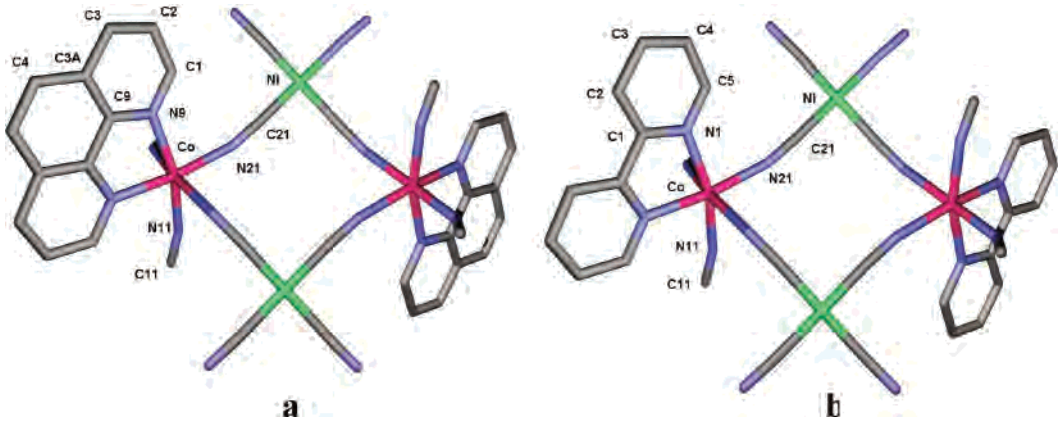

Figure 2. View of the four-metal-membered fused rings that form the two-dimensional structural motif in the isostructural compounds (a) **1** and (b) **2**. Co(II) and Ni(II) centers are in purple and green, respectively.

bridged Fe(II)−Cu(I) systems.[3,4] It has commonly been assumed that cyanide groups from the dissociation of $[Fe(CN)_6]^{3-}$ are responsible for the reduction process, yielding cyanogen as the oxidation product.[2,3] If $[Co(CN)_6]^{3-}$ were used in similar hydrothermal conditions, in principle, the formation of Co(II)-containing species would be expected. Bearing this in mind, we have employed hexacyanocobaltate(III) and Ni(II) ions to successfully obtain cyano-bridged Co(II)−Ni(II) complexes. In the course of the hydrothermal reaction, free cyanide anions from the dissociation of the hexacyanocobaltate units react with the Ni(II) ions to form highly stable $[Ni(CN)_4]^{2-}$ moieties and, as a consequence, the diimine ligands are forced to coordinate to the Co(II) ions. Finally, the assembly of the $[Co(diimine)_n]^{2+}$ and $[Ni(CN)_4]^{2-}$ building blocks leads to complexes **1**−**3**. Note that this sequence of steps may not represent the true reaction mechanism, yet only a logical order. Because the organic polytopic ligands (phen and 2,2′-bipy) are poorly soluble in water, the hydrothermal conditions (high temperature and pressure) are essential for the dissolution of the metal−ligand suspension and then for the crystallization, during cooling, of complexes **1**−**3**. It should be noted that a change in the reaction time has also a direct influence on the nature (stoichiometry and structure) of the final product. Thus, the reaction of $NiCl_2 \cdot 6H_2O$, $K_3[Co(CN)_6]$, and phen in a 1:1:1 molar ratio, at 180 °C and under autogenous pressure for 2 h, gives rise to the $[Ni(CN)_4Co(phen)]$ two-dimensional bimetallic system, **1**. By using $NiCl_2 \cdot 6H_2O$, $K_3[Co(CN)_6]$, and 2,2′-bipy instead of phen in the same reaction conditions, ′**2**, isostructural with **1**, is obtained. At variance, the hydrothermal reaction among $NiCl_2 \cdot 6H_2O$, $K_3[Co(CN)_6]$, and 2,2′-bipy in the same molar ratio as that above, at the same temperature but using a longer reaction time (12 h), results in the formation of the one-dimensional bimetallic complex **3**.

In **1** and **2**, the diimine ligands act as passivating agents by blocking two metal-coordination sites, while cyanide ligands favor the propagation of the structure into a two-dimensional network. In **3**, with increasing reaction time, an additional chelating donor ligand (2,2′-bipy) coordinates the metal center, so that four cobalt-coordination sites are blocked by the diimine ligands. The structure can thus propagate in just one dimension and contains bimetallic zigzag chains.

Crystal Structures of 1 and 2. The asymmetric units of the monoclinic compounds $[Ni(CN)_4Co(L)]$ (L = phen, **1**; L = 2,2′-bipy, **2**) are composed of one Ni(II) ion and one Co(II) ion, lying about a crystallographic inversion center and a crystallographic 2-fold axis, respectively (4a and 4e Wyckoff positions, respectively), half a heteroaromatic ligand (lying about a 2-fold axis, e Wyckoff position), and two cyanide moieties. Each Co(II) center shows a distorted octahedral stereochemistry, of idealized C_{2v} symmetry (Figure 2): two cis positions are occupied by the nitrogen atoms of one chelating diimine ligand [$Co-N_L$ 2.157(1) (**1**) and 2.175(7) (**2**) Å; N_L-Co-N_L 76.70(7)° (**1**) and 76(1)° (**2**)].

In both **1** and **2**, the four remaining coordination positions of the Co(II) ions are occupied by the nitrogen atoms of the cyanide groups belonging to four distinct $[Ni(CN)_4]^{2-}$ moieties [$Co-N_{cyano}$ 2.069(1) and 2.211(1) Å (**1**), 2.11(1) and 2.15(1) Å (**2**)]. Because of the trans labilizing effect of opposite cyanide groups, at least in the case of **1**, $Co-N_{cyano}$ distances are shorter for the CN^- group trans to the nitrogen atoms of the L ligand.

At variance, as shown in Figure 2, the Ni(II) centers show a square-planar coordination [$Ni-C_{cyano}$ 1.860(2) and 1.879(2) Å, $C_{cyano}-Ni-C_{cyano}$ 90.91(7)° in **1**; $Ni-C_{cyano}$ 1.87(1) and 1.96(1) Å, $C_{cyano}-Ni-C_{cyano}$ 90(1)° in **2**].

Thus, in both compounds, each crystallographically independent cyanide group acts as a bridge between two distinct Ni(II) and Co(II) metal ions [4.9368(4) or 5.0086(4) Å apart in **1** and 4.951(2) or 5.006(2) Å in **2**] allowing a two-dimensional, corrugated layer to be created in the *ac* plane (Figure 3). From a different point of view, it could be said that the $[Ni(CN)_4]^{2-}$ moieties allow the Co(II) magnetic centers [6.5604(4), the *a* axis, or 7.4752(7) Å apart in **1** and 6.6089(2) or 7.446(4) Å in **2**] to enter into contact. The two-dimensional layers are formed by four-metal-membered fused rings, with the metal ions alternating with each other within a single ring. Polymerization in the third dimension is hampered by the presence of the diimine ligands, acting, as expected from their common N,N′-endo-bidentate coordination mode, as passivating agents. Pairs of parallel L ligands, separated by a distance of 6.5604(4) (**1**) or 6.6089(2) (**2**) Å

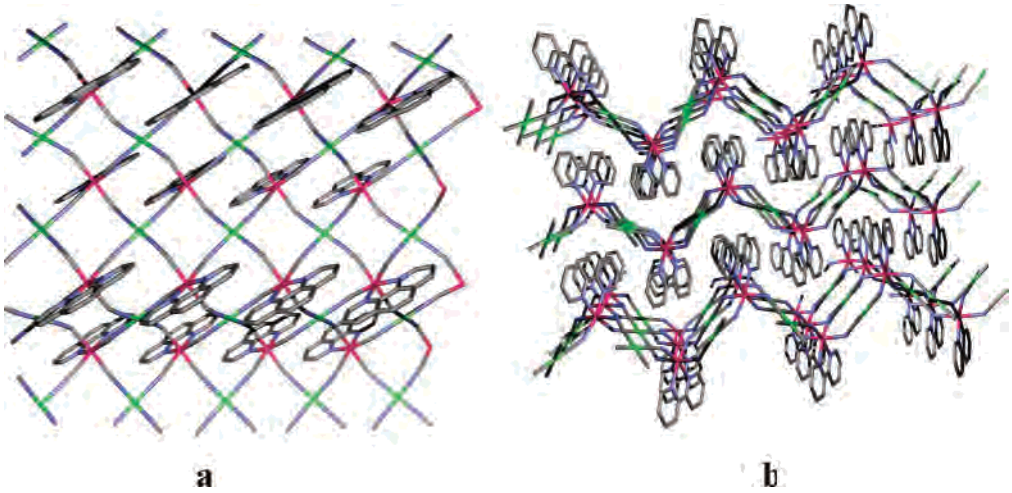

Figure 3. Representation of the two-dimensional corrugated layer in the isostructural compounds (a) **1** and (b) **2** as viewed approximatively down [010] and [100], respectively. Co(II) and Ni(II) centers are in purple and green, respectively.

(the full length of the *a* axis), emerge alternately from both sides of the layers, with their longest inertial axis being directed about the [1, 0, 1] direction.

In both compounds, the formation of the two-dimensional layers implies a certain distortion at every joint between the $[Ni(CN)_4]^{2-}$ moieties and the Co(II) ions, especially for one of the two independent cyanide groups: indeed, while the $Ni-C_{cyano}-N_{cyano}$ angles do not deviate significantly from linearity [174.8(2) and 176.2(1)° in **1** and 177.5(9) and 177.6(8)° in **2**], equatorial[16] $Co-N_{cyano}-C_{cyano}$ angles of 163.17(15)° (**1**) and 157.5(9)° (**2**) are observed, while higher distortions are necessary in order to allow coordination at the axial sites [axial $Co-N_{cyano}-C_{cyano}$ 143.69(15)° (**1**) and 138.4(2)° (**2**)].

If the four cyanide ligands bonded to the Co(II) ions were situated in their equatorial plane, we could retrace our structural motif to that of the host of the Hofmann-type clathrates,[17] of which **1** and **2** may be considered a distortion.[18] An analogous two-dimensional structural motif has already been found in the isostructural species $[Ni(CN)_4Cd(2,2'\text{-bipy})]$[19] and $[Pt(CN)_4Cu(2,2'\text{-bipy})]$,[20] where, along the fused rings, pseudo-octahedral Cd(II)−Cu(II) ions alternate with square-planar Ni(II)−Pt(II) ones. It is worth noting that, in these cases as well, the cyanide groups coordinate with their carbon atoms to the square-planar metal center.

Crystal Structure of 3. The asymmetric unit of the orthorhombic species **3** is composed of one Ni(II) ion and one Co(II) ion, lying about a crystallographic inversion center and a crystallographic 2-fold axis, respectively (4a and 4c Wyckoff positions, respectively), one crystallographically independent 2,2′-bipy ligand, and two crystallographically independent cyanide groups. As in **1** and **2**, the Ni(II) ion shows a slightly distorted square-planar stereochemistry (Figure 4), being connected to the carbon atoms of four distinct cyanide moieties [$Ni-C_{cyano}$ 1.858(4) and 1.869(6) Å; $C_{cyano}-Ni-C_{cyano}$ 92.0(2)°]. The Co(II) ion, though hexacoordinated and of idealized C_{2v} symmetry, shows a different CoN_6 environment than that in **1** and **2** (Figure 4): four coordination positions are occupied by two chelating 2,2′-bipy ligands, acting in the N,N′-endo-bidentate mode [$Co-N_{bipy}$ 2.075(4) and 2.117(3) Å; $N_{bipy}-Co-N_{bipy}$ 77.9(1) (endocyclic) and 94.2(1)°]. The remaining two cis coordination positions are occupied by the nitrogen atoms of two cyanide groups belonging to two distinct $[Ni(CN)_4]^{2-}$ moieties [$Co-N_{cyano}$ 2.083(3) Å; $N_{cyano}-Co-N_{cyano}$ 93.3(2)°].

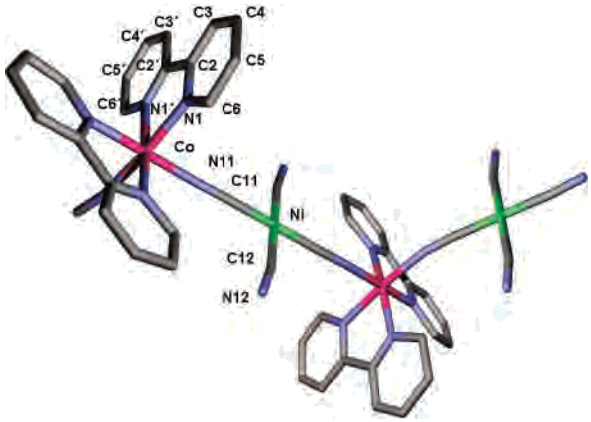

Figure 4. View of the portion of a fragment of the one-dimensional structural motif in **3**. Co(II) and Ni(II) centers are in purple and green, respectively.

Notably, unlike in the case of **1** and **2**, just one crystallographically independent cyanide group acts as a bridging ligand [C−N 1.145(5) Å vs 1.133(7) Å for the terminal cyanide one]. No evident distortions can be observed in this case at the joints between the $[Ni(CN)_4]^{2-}$ moieties and the Co(II) ions: both the bridging and the terminal cyanide groups substantially preserve their linearity [$Co-N_{cyano}-C_{cyano}$ 170.1(3)°; $Ni-C_{cyano}-N_{cyano}$ 175.5(4) and 175.8(5)°].

Because four coordination sites on the Co(II) ion are blocked by the 2,2′-bipy ligands, bridging by the cyanide

(16) The equator is here defined by the Co(L) plane.
(17) Iwamoto, T.; Nakano, T.; Morita, M.; Miyoshi, T.; Miyamoto, T.; Sasaki Y. *Inorg. Chim. Acta* **1968**, *2* (3), 313.
(18) Hofmann's clathrates are based upon octahedral $Ni(CN)_4(L)_2$ chromophores (typically, L = ammonia), with the L ligands trans to each other. At variance, the geometrical requirement of cis coordination by 2,2′-bipy and phen in **1** and **2** forces a corrugated, rather than a planar, two-dimensional network of pseudosquare meshes.
(19) Hashimoto, M.; Iwamoto, T. *Acta Crystallogr.* **1994**, *C50*, 496.
(20) Falvello, L. R.; Garde, R.; Tomás, G. *J. Cluster Sci.* **2000**, *11*, 125.

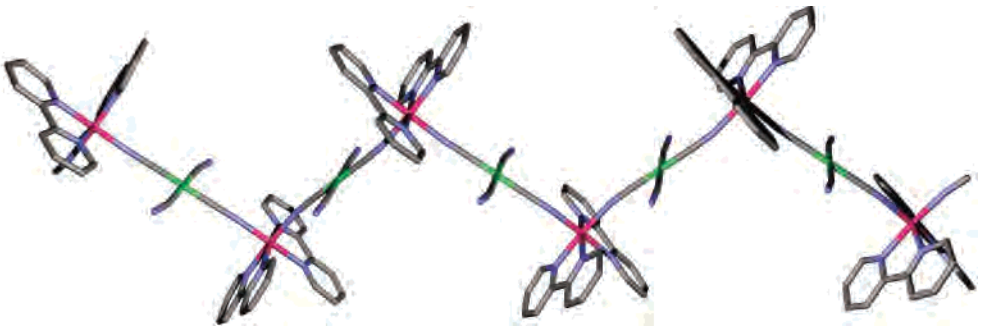

Figure 5. Representation of the one-dimensional zigzag chain motif in ′**3.** Co(II) and Ni(II) centers are in purple and green, respectively.

moieties allows polymerization just in one dimension: one-dimensional zigzag chains are indeed present about *c* (Figure 5).

The same structural motif has been previously observed in the isostructural *homometallic* $[Ni_2(CN)_4(2,2'\text{-bipy})_2]$ species, in which Ni(II) ions occupy both the pseudo-octahedral and the square-planar coordination positions along the one-dimensional zigzag chains.[21] Being that the ionic radii of the hexacoordinated Ni(II) and Co(II) centers are nearly equal (0.69 vs 0.65 Å), (i) the *V*/*Z* values of **3** and $[Ni_2(CN)_4(2,2'\text{-bipy})_2]$ are almost identical (ca. 567 vs 564 Å^3, respectively) and (ii) their *c* axes, parallel to the translation axis of the polymers, thus determining their pitch, are highly comparable [15.818(3) vs 15.755(1) Å].

Along the chain of **3**, Ni(II) and Co(II) centers alternate at a distance of 5.054(2) Å, implying *intra*chain Co(II)···Co(II) distances of about 10.10 Å, while shortest *inter*chain Co(II)···Co(II) distances of 8.694(3) Å can be envisaged.

Comparative Structure Analysis. Polymeric species similar to **1**−**3** are known in the literature and can be structurally compared with the title compounds. In the presence of at least one 2,2′-bipy moiety on one metal center, polymerization has been reached just in a few cases: (a) in heterobimetallic $[Fe(bipy)(CN)_4]Ni(1,3\text{-diaminopropane})\cdot 3H_2O$, in which octahedral Fe(II) ions are connected, by bridging cyanides, to trans D_{4h} Ni(II) centers;[22] (b) in the isostructural $[Fe(bipy)(CN)_4]_2M(H_2O)\cdot MeCN\cdot 0.5H_2O$ [M = Mn(II) and Co(II)] corrugated double-stranded chains[23] (with the M(II) ions connected to five [M−Fe(III)]-bridging cyano groups and to a water molecule), and (c) in $[Cr(bipy)(CN)_2]_2Mn(CN)_4(H_2O)_2$ (also containing double-stranded chains).[24] Similar structural motives are also found in $[Fe(bipy)(CN)_4]_2Zn$[25] (sharing the same space group and comparable unit cell parameters with the solvated $[Fe(bipy)(CN)_4]_2M(H_2O)\cdot MeCN\cdot 0.5H_2O$ species) and in $[Fe(bipy)(CN)_4Co(H_2O)_2]\cdot 4H_2O$.[26]

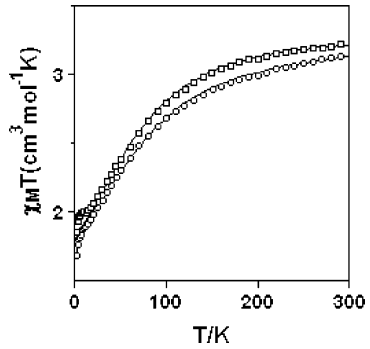

Figure 6. Temperature dependence of the $\chi_M T$ product for complexes **1** (circles) and **3** (squares) in the temperature range 2−300 K and in a field of 0.6 T. The solid lines represent the best fits with Δ positive.

With regards to phen-containing compounds, to our knowledge, species **1** is the first example of a cyanide-bridged *polymeric* structure showing the 1,10-phenanthroline ligand chelating the Co(II) ion. Actually, one-dimensional polymers have been previously found in the presence of the Cu(I) ion (as in the case of the *homometallic* helix of $[Cu(\mu_2\text{-CN})(phen)]$)[27] or in $[Cr(phen)(CN)_2]_2Mn(CN)_4(H_2O)_2\cdot 4H_2O$ (and in its Fe(III)−Cu(II) analogue, both isostructural with the above-mentioned $[Cr(bipy)(CN)_2]_2Mn(CN)_4(H_2O)_2$ polymer). Co(II) ions have indeed been employed in the synthesis of a number of heterobimetallic species, yet only oligonuclear compounds have resulted: see, e.g., the trinuclear $[CoW_2(\mu_2\text{-CN})(CO)_{10}(phen)_2]\cdot CH_2Cl_2$[28] or the pentanuclear $[Fe_2Co_3(\mu_2\text{-CN})_6(CN)_6(tetramephen)_6]\cdot 9H_2O$[29] species (tetramephen = 3,4,7,8-tetramethyl-1,10-phenanthroline).

Magnetic Properties. The temperature dependence of the $\chi_M T$ product for complexes **1**−**3** in the temperature range 2−300 K at a magnetic field of 0.6 T is given in Figures 6 and 7. The $\chi_M T$ values for **1**−**3** at room temperature are 3.16, 3.24, and 2.99 cm^3 mol^{-1} K, respectively. These values substantially exceed the spin-only value for a high-spin cobalt(II) ($S = {}^3/_2$, 1.875 cm^3 mol^{-1} K with $g = 2$) but are close to the value expected when the spin momentum and the angular momentum exist independently (3.37 cm^3 mol^{-1}

(21) Cernak, J.; Abboud, K. A. *Acta Crystallogr., Sect. C* **2000**, *56*, 783.
(22) Chang, F.; Sun, H.-L.; Gao, S. *Chin. J. Inorg. Chem.* **2002**, *18*, 95.
(23) Toma, L. M.; Lescouezec, R.; Lloret, F.; Julve, M.; Vaissermann, J.; Verdaguer, M. *Chem. Commun.* **2003**, 1850.
(24) Toma, L. M.; Lescouezec, R.; Vaissermann, J.; Delgado, F. S.; Ruiz-Perez, C.; Carrasco, R.; Lloret, F.; Julve, M. *Chem. Eur. J.* **2004**, *10*, 6130.
(25) Lescouezec, R.; Lloret, F.; Julve, M.; Vaissermann, J.; Verdaguer, M. *Inorg. Chem.* **2002**, *41*, 818.
(26) Lescouezec, R.; Vaissermann, J.; Ruiz-Perez, C.; Lloret, F.; Carrasco, R.; Julve, M.; Verdaguer, M.; Dromzee, Y.; Gatteschi, D.; Wernsdorfer, W. *Angew. Chem., Int. Ed.* **2003**, *42*, 1483.
(27) Dyason, J. C.; Healy; P. C.; Engelhardt, L. M.; Pakawatchai, C.; Patrick, V. A.; White, A. H. *J. Chem. Soc., Dalton Trans.* **1985**, 839.
(28) Sheng, T.; Vahrenkamp, H. *Inorg. Chim. Acta* **2004**, *357*, 1739.
(29) (a) Berlinguette, C. P.; Dragulescu-Andrasi, A.; Sieber, A.; Galan-Mascaros, J. R.; Gudel, H.-U.; Achim, C.; Dunbar, K. R. *J. Am. Chem. Soc.* **2004**, *126*, 6222. (b) Berlinguette, C. P.; Galan-Mascaros, J. R.; Dunbar, K. R. *Inorg. Chem.* **2003**, *42*, 3416. (c) Berlinguette, C. P.; Vaughn, D.; Canada-Vilalta, C.; Galan-Mascaros, J. R.; Dunbar, K. R. *Angew. Chem., Int. Ed.* **2003**, *42*, 1523.

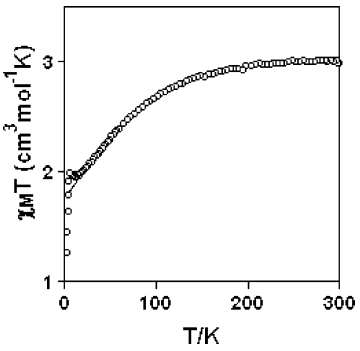

Figure 7. Temperature dependence of the $\chi_M T$ product for complex **2** in the temperature range 2−300 K and in a field of 0.6 T. The solid line represents the best fit with Δ positive.

K). This is indicative of an unquenched orbital contribution, typical of the $^4T_{1g}$ ground state. For **1**−**3**, $\chi_M T$ gradually decreases with the temperature until about 15 K. The high-temperature behaviors (>15 K) are typical of a magnetically isolated six-coordinated high-spin cobalt(II) ion with spin−orbit coupling in the $^4T_{1g}$ ground state. The rapid decrease for **1** below 15 K suggests the possibility of very weak intralayer and/or interlayer antiferromagnetic interactions, with the former taking place through the diamagnetic $[Ni(CN)_4]^{2-}$ bridging groups, which are known to be very poor mediators of the magnetic interactions.[30] Below 15 K, complexes **2** and **3** seem to show a magnetic behavior different from that of **1**. Indeed, when the temperature is lowered, the $\chi_M T$ product first remains constant, or even increases with a magnetic field of 300 G, and then decreases sharply down to 2 K. ac magnetic susceptibility measurements do not reveal any peak, and hence the upturn of $\chi_M T$ below 15 K is not due to magnetic ordering. It should be noted that a similar behavior has been observed for other cobalt(II) complexes.[31] Although the origin of this behavior remains at the moment unknown, some authors have suggested that it results from the complicated energy dependence of the resulting Zeeman levels, probably influenced also by weak exchange coupling.[31a] As in **1**, the sharp decrease of $\chi_M T$ at very low temperatures is due to intralayer and/or interlayer antiferromagnetic interactions.

In a purely O_h symmetry, the $^4T_{1g}$ ground state (which is well separated from the single ion excited state $^4T_{2g}$ by about 9000 cm^{-1}) splits by spin−orbit coupling into a sextet, a quartet, and a Kramers doublet. The Hamiltonian describing the spin−orbit coupling is given by

$$-3/2\kappa\lambda\mathbf{LS}$$

where κ and λ are the orbital reduction and spin−orbit coupling parameters, respectively. The factor −3/2 is due to the use of the T−P isomorphism, in which the angular momentum for the $^4T_{1g}$ state is equal to the angular momentum of the ^4P free ion state multiplied by −3/2. However, for real compounds, the distortion around the cobalt(II) ions must be considered. Under an axial distortion, the triplet $^4T_{1g}$ ground state splits into an orbital singlet $^4A_{2g}$ and an orbital doublet ^4E_g, with the energy gap between them being the axial splitting parameter, Δ (see Chart 1).

Chart 1

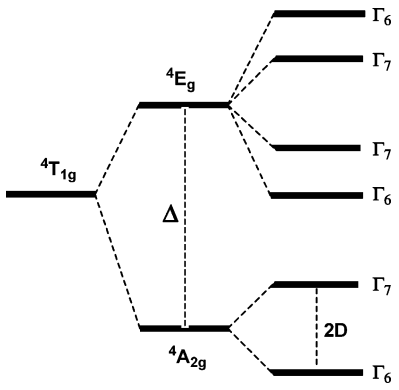

The one-center operator responsible for an axial distortion can be expressed as

$$H_{ax} = \Delta(\mathbf{L}_z^2 - 2/3)$$

It should be noted that the axial parameter Δ can be used in both the trigonal and tetragonal fields.[32]

The $^4A_{2g}$ and ^4Eg levels split by spin−orbit coupling give rise to two and four Kramers doublets, respectively. The energy gap between the two Kramers doublets arising from the $^4A_{2g}$ state, Γ_6 and Γ_7, is defined as $2D$.

The full Hamiltonian involving spin−orbit coupling, axial distortion, and Zeeman interactions takes the form

$$\mathbf{H} = \Delta(\mathbf{L}_z^2 - 2/3) + (-3/2)\kappa\lambda\mathbf{LS} + \beta[-(3/2)\kappa\mathbf{L} + g_e\mathbf{S}]H$$

Spin−orbit coupling and distortion were diagonalized together by solving the 12 × 12 secular matrix. The resulting Zeeman coefficients for the two directions parallel and perpendicular to the magnetic field were included in the van Vleck equation to obtain the expression for the average magnetic susceptibility. Owing to the complicated magnetic behavior observed for **2** and **3** below 15 K, we have not included a θ parameter to take into account intermolecular interactions. The fit of the experimental data to the theoretical equation shows that the sign of Δ cannot be unambiguously determined from the powder susceptibility data because the agreement factors (R) for positive and negative Δ values for each compound are very close. The best-fit parameters for both positive and negative Δ values were $\kappa = 1.0$, $\lambda = -172$, $\Delta = 671$ cm^{-1}, $R = 2 \times 10^{-5}$ and $\kappa = 0.88$, $\lambda = -153$, $\Delta = -404$ cm^{-1}, $R = 3.9 \times 10^{-5}$ for **1**, $\kappa = 1.0$, $\lambda = -140$, $\Delta = 486$, $R = 1.1 \times 10^{-4}$ and $\kappa = 0.86$, $\lambda = -153$, $\Delta = -558$ cm^{-1}, $R = 1.5 \times 10^{-5}$ for **2**, and $\kappa = 1.0$, $\lambda = -165$, $\Delta = 743$ cm^{-1}, $R = 8 \times 10^{-5}$ and $\kappa = 0.88$, $\lambda = -165$, Δ

(30) (a) Muga, I.; Gutiérrez-Zorrilla, J. M.; Vitoria, P.; Román, L.; Lezama, P.; Beitia, J. I. *Eur. J. Inorg. Chem.* **2004**, *43*, 1886. (b) Smekal, Z.; Travnicek, Z.; Mrozinski, J.; Marek, J. *Inorg. Chem. Commun.* **2003**, *6*, 1395.

(31) Raebiger, J. W.; Manson, J. L.; Sommer, R. D.; Geiser, U.; Rheingold, A. L.; Miller, J. S. *Inorg. Chem.* **2001**, *40*, 2578. (b) van der Werff, P. M.; Batten, S. R.; Jensen, P.; Moubaraki, B.; Murray, K. S.; Tan, E. H.-K. *Polyhedron* **2001**, *20*, 1129.

(32) Figgis, B. N.; Lewis, J.; Maabs, F. E.; Webb, G. A. *J. Chem. Soc. A* **1966**, 1411.

$= -668\ cm^{-1}$, $R = 1.8 \times 10^{-5}$ for **3**. These fitting parameters are in good accordance with previously reported values for distorted octahedral Co(II) complexes.[33] The Δ values obtained for complexes **1**−**3** indicate low distortion in agreement with the high magnetic moment at room temperature. The λ values are slightly smaller than that for the free ion ($\lambda_0 = -180\ cm^{-1}$) due to covalent effects.

When Δ is large enough and positive, only the two lowest Kramers doublets arising from the $^4A_{2g}$ ground term, Γ_6 and Γ_7, are thermally populated. Then, the energy gap between these two Kramers doublets can be considered as an axial zero-field splitting (ZFS) within the quartet state.

In this case, the magnetic properties may be interpreted by using the Hamiltonian:

$$\mathbf{H} = D(\mathbf{Sz}^2 - 5/4) + \beta \mathbf{S} g H$$

with $2D$ being, as indicated above, the energy separation between Γ_6 and Γ_7. From this Hamiltonian, the following expression can be drawn:[34]

$$\chi_{ZFS} = \frac{Ng^2\beta^2}{k_B T}\left[\frac{1}{3}\frac{1 + 9e^{-2x}}{4(1 + e^{-2x})} + \frac{2}{3}\frac{1 + \frac{3k_B T}{4D}(1 - e^{-2x})}{1 + e^{-2x}}\right]$$

where $x = D/k_B T$. If we assume that complexes **1**−**3** have positive Δ values, the parameters obtained from the best fit are $|D| = 116(5)\ cm^{-1}$ and $g = 2.630(8)$ for **1**, $|D| = 107(4)\ cm^{-1}$ and $g = 2.662$ (8) for **2**, and $|D| = 92(2)\ cm^{-1}$ and 2.577(4) for **3**. In this case, the influence of the angular momentum has been incorporated into D and g. It should be noted that the $2D$ values for the axial ZFS are similar to those of 210, 180, and 175 cm^{-1} for **1**−**3**, respectively, obtained from the matrix diagonalization method.

At 2 K, complexes **1**−**3** show magnetization saturation values, M_s, of 2.20, 2.27, and 2.19 $N\beta$, which are smaller that the M_s expected value for $S = {}^3/_2$ systems with $g = 2$. The differences are due to the fact that only the ground Kramers doublet is populated at 2 K, to which an effective spin $S_{eff} = {}^1/_2$ with a $g = (10 + 3\kappa)/3$ can be associated. The calculated value 2.16 $N\beta$ is close to the experimental values for **1**−**3**.

Concluding Remarks

The results reported here clearly show that the hydrothermal synthesis is a powerful and versatile tool for preparing cyano-bridged bimetallic materials. Up to now, only fully reduced cyano-bridged Fe(II)−Cu(I) systems were successfully obtained by hydrothermal techniques, employing $[Fe(CN)_6]^{3-}$ as a precursor together with a copper(II) salt and polytopic ligands. We have shown here that the same strategy can be extended to prepare cyano-bridged Co(II)−Ni(II) networks. Unfortunately, square-planar $[Ni(CN)_4]^{2-}$ anions are diamagnetic, so that the magnetic properties are only characterized by very weak, if any, magnetic interactions between Co(II) ions. Hydrothermal reactions of $[Mn(CN)_6]^{3-}$ anions with Co(II) or Mn(II) ions in the presence of capping ligands are currently being examined in our laboratory, with the aim of obtaining cyano-bridged extended systems, in which all metal centers are paramagnetic.

Acknowledgment. This work was supported by the Spanish Ministerio de Ciencia y Tecnología through Projects BQU2001/3221 and Junta de Andalucía. A.R. thanks the Ministerio de Ciencia y Tecnología for a predoctoral fellowship. Financial support from the Fondazione Provinciale Comasca is also acknowledged.

IC0511672

(33) Colacio, E.; Lloret, F.; Maimoun, I. B.; Kivekäs, R.; Sillapää, R.; Suárez-Varela, J. *Inorg. Chem.* **2003**, *42*, 2720.
(34) Telser, J.; Drago, R. S. *Inorg. Chem.* **1985**, *24*, 4765.